CrystEngComm

Coordination polymers based on pyrazole-4-carboxaldehyde-containing Cu_3N_6 metallacycles as building units.

Journal:	*CrystEngComm*
Manuscript ID	CE-ART-03-2019-000421.R1
Article Type:	Paper
Date Submitted by the Author:	08-Apr-2019
Complete List of Authors:	Kreiger, David; Florida International University, Chemistry and Biochemistry Mathivathanan, Logesh; Florida International University , Department of Chemistry & Biochemistry Raptis, Raphael; Florida International University, Chemistry and Biochemistry

Journal Name

ARTICLE

Coordination polymers based on pyrazole-4-carboxaldehyde-containing Cu_3N_6 metallacycles as building units

Received 00th January 20xx,
Accepted 00th January 20xx

DOI: 10.1039/x0xx00000x

www.rsc.org/

David I. Kreiger, Logesh Mathivathanan, and Raphael G. Raptis *

Five crystal structures containing trinuclear Cu(II)-4-fomyl pyrazolato units are reported: a 0-D Cu_3 complex (**1**) was prepared in the presence of terminal chloride ligands, a 3D polymer with **dia** topology and 3-fold interpenetrated structure (**2**) involved 1,2-bipyridylethylene (bpe) linkers, while a second 1-D polymer (**3**) formed by linking SBUs via formyl group coordination. Two 3D polymers (**4** and **5**) with novel topologies consist of 14-nodal $3^8,4^2,5^4$-c and 3-nodal 3,3,4-c nets, respectively.

Introduction

The coordination chemistry of carbonyl compounds has been focused on carboxylic acids, and less frequently on amides. In contrast, ketones and aldehydes seldom feature in coordination complexes, except when completing a chelate bite. For example, pyridine-2-carboxaldehyde is a common chelate, whereas pyridine-bis-2,6-carboxaldehyde has been used as a pincer ligand for metals in labile oxidation states.[1–5] Aromatic aldehydes, e.g., benzaldehyde, tend to form few first row, σ-bonded coordination complexes, except with Zn(II).[2,6–15] In a few cases, aldehydes bind Zn(II) stronger than some anionic ligands.[16,17] A search in the Cambridge Structural Database (CSD) for coordinated aldehydes (with H-atoms on β-carbons) turns up approximately one hundred crystal structures, of which fewer than one half involve first row transition metal complexes with either a σ- or π-,η^2-bound aldehyde. Some of the frequently encountered Zn-aldehyde complexes have been studied as models of liver alcohol dehydrogenase (LADH).[18,19] Magnetic exchange mediated by bridging, σ-bound –CH(O) groups has been described in a manganese 2D-coordination polymer [O-Mn: 2.197(7) Å].[15] To the best of our knowledge, only four coordination polymers containing CH(O)-bound Cu centers have been reported: Two containing only fairly long Cu-O contacts of 2.723(7) Å[2] and 2.877(3) Å,[20] while significantly shorter Cu-O bonds of 2.296(6) Å and 2.005(4) Å were measured in the other two.[21,22] Polynuclear Cu(II)-pyrazolato cluster chemistry is rich with nuclearities ranging from two to 34.[23] 4-Subsituted pyrazolates typically yield trinuclear metallacycles: We and others have published pyrazolato complexes of the general formula $[Cu_3(\mu_3\text{-E})(\mu\text{-4-R-pz})_3X_3]^z$, where E = O, OH, Cl_2, Br_2, OMe, OEt; R = H, Cl, Br, NO_2, Me, Ph, CH(O); X = Cl, Br, SCN, NO_2, CF_3CO_2, PhCOO, py and z = 1-, 2-, 1+ or 2+.[24–28] The trinuclear subunits can also be strung together as secondary building units (SBUs) with suitable linkers to form 1D-chains, 2D-sheets and 3D-lattices.[29] We have also reported the pyrazole-4-carboxaldehyde-containing, 0D-complex $(PPN)_3[Cu_3(\mu_3\text{-O})(\mu\text{-4-CH(O)-pz})_3Cl_3]Cl$.[24] Here, we are now showing that, in the absence of other terminal or bridging ligands, 4-CH(O)-pz^- can be used as a $\mu_{\text{⎚}},\eta^3$-linker by itself to form extended networks. Specifically, we are reporting three new coordination polymers (CPs), **3**, **4** and **5**, constructed by assemblies of $[Cu^{II}_3(\mu_3\text{-OH})(\mu\text{-4-CH(O)-pz})_3]^{2+}$ cations clipped together by short intermolecular Cu-(O)HC bonds, along with the corresponding Cl-terminated SBU, **1**, and one bipyridine-linked MOF, **2**. Topological, geometrical and 3D-structural properties of four extended network compounds are also discussed.

Experimental

Materials and Methods

$CuCl_2.2H_2O$, $Cu(ClO_4)_2.6H_2O$, tetraphenylphosphonium chloride, 1,2-bispyridylethylene (1,2-bpe, Acros), $Cu(CF_3SO_3)_2$ (Alfa-Aesar), and 4-CH(O)-pzH (Combi Blocks, Inc.) were purchased from commercial sources and used without further purification. Solvents were purified using standard procedures. All reactions were conducted open to the atmosphere.

Department of Chemistry and Biochemistry, Florida International University, 11200 SW 8th St, Miami, FL. 33199. USA.
† Footnotes relating to the title and/or authors should appear here.
Electronic Supplementary Information (ESI) available: Infrared spectra of **2**, **3** and **5** (S1-S3), ^{1}H-NMR spectrum of **5** (S4). CCDC 1880271-1880275. See DOI: 10.1039/x0xx00000x

Table 1. Crystallographic details for Compounds 1 - 5.

Crystal Parameters					
Compound	**$(Ph_4P)_2$[1]**	**[2]$(CF_3SO_3)_2$**	**[3]$(CF_3SO_3)_2$**	**[4]$(CF_3SO_3)_2$**	**[5]$(ClO_4)_2$**
Formula	$C_{60}H_{49}Cl_3Cu_3N_6O_4P_2$	$C_{62}H_{49}Cu_3F_6N_{14}O_{13}S_2$	$C_{28}H_{20}Cu_6F_{12}N_{12}O_{29}S_4$	$C_{38}H_{40}Cu_6F_{12}N_{14}O_{20}S_4$	$C_{12}H_9Cl_2Cu_3N_6O_{12}$
f_w (amu)	1276.96	1566.89	1726.04	1740.24	689.78
Temperature (K)	293(2)	296(2)	296(2)	293(2)	296(2)
Size (mm^3)	0.31 x 0.12 x 0.05	0.27 x 0.26 x 0.23	0.10 x 0.17 x 0.17	0.54 x 0.46 x 0.24	0.28 x 0.28 x 0.18
Crystal System	Triclinic	Monoclinic	Monoclinic	Orthorhombic	Cubic
Space group	$P\bar{1}$	$C2/c$	$P2_1/n$	$Pna2_1$	$I\bar{4}3d$
a (Å)	12.858(1)	11.903(1)	18.9259(8)	17.989(1)	23.8296(8)
b (Å)	13.770(1)	25.050(2)	15.1550(7)	17.989(1)	23.8296(8)
c (Å)	18.617(2)	23.801(2)	20.6283(9)	24.289(2)	23.8296(8)
α (°)	76.345(1)	90	90	90	90
β (°)	75.103(1)	97.605(1)	91.700(1)	90	90
γ (°)	66.284(1)	90	90	90	90
V ($Å^3$)	2883.3(4)	7034(1)	5914.0(5)	7860.3(8)	13531.6(1)
Z	2	4	4	4	16
ρ_{calc} (g cm^{-3})	1.471	1.480	1.936	1.471	1.354
μ (mm^{-1})	1.343	1.044	2.390	1.792	2.074
Total data	33257	40230	1574738	146084	140252
Unique data (R_{int})	13010 (0.0285)	8364 (0.0252)	12220 (0.0441)	16148 (0.0351)	2327 (0.0488)
2θ range (°)	3.832 to 55.312	4.00 to 46.48	5.728 to 53.01	5.518 to 52.92	6.398 to 52.832
Goodness of fit (GOF) on F^2	1.025	1.034	1.040	1.038	1.068
R_1/wR_2 ($I > 2\sigma(I)$)	0.0393/0.0970	0.0637/0.1799	0.0508/0.1384	0.0371/0.0935	0.0349/0.0930
R_1/wR_2 (all data)	0.0679/0.1104	0.0817/0.1961	0.0673/0.1510	0.0416/0.0970	0.0383/0.0963

Single-crystal X-ray Crystallography

Single crystals of the compounds were mounted on a MiteGen CryoLoop or on a glass fiber and diffraction data were collected on a Bruker D8 Quest diffractometer equipped with a Photon 100 CMOS, or a Bruker APEX II diffractometer with a SMART detector, using Mo-Kα radiation. Data were collected using the APEX 3 or APEX 2 suite; structure solution was obtained using intrinsic phasing with SHELXT.[30] Data were refined by least-square methods available within SHELXL[31] using the Olex2 interface.[32] Electron densities corresponding to disordered interstitial solvent molecules were accounted for by using the MASK routine available within Olex2.

X-ray Powder Diffraction

Powders of samples were loaded in a capillary and mounted on the Bruker D8 Quest diffractometer and 360º phi-scan images were collected. The scans were integrated using Fit2D to obtain powder patterns.[33,34]

Topology

Topological analysis was performed with the ToposPro program package and the TTD collection of periodic network topologies.[35]

Void Volume

Solvent accessible void volumes for $\mathbf{2^{2+}}$, $\mathbf{4^{2+}}$ and $\mathbf{5^{2+}}$ were calculated using the Mercury program package.[36]

IR data

ATR-IR data were collected using an Agilent Technologies Cary 600 Series FTIR Spectrometer with 16 scans from 4000-500 cm^{-1}. Data were analyzed using Spectragryph 1.2.10 software.[37] Powdered samples were placed on the ATR stage and data were collected, then minimal acetonitrile was added to dissolve the compounds and data were collected from the resulting solutions.

Thermogravimetric Analysis

TGA was performed with a TA instruments SDT Q600 from RT to 900 °C at a heating rate of 5 °C/min with He as the carrier gas. The data are included in the Supporting Information.

Synthesis

$(Ph_4P)_2[Cu_3(\mu_3\text{-}O)(\mu\text{-}4\text{-}CH(O)\text{-}pz)_3Cl_3]$, $(Ph_4P)_2$[1]

Complex **$(Ph_4P)_2$[1]** was prepared similarly to the previously published **$(PPN)_2$[1]** (PPN = $(Ph_3P)_2N^+$.[24] $CuCl_2.2H_2O$ (1 mmol, 170.5 mg), 4-CH(O)-pzH (1 mmol, 96.1 mg) NaOH (2 mmol, 80 mg, and Ph_4PCl (0.66 mmol, 262.4 mg) were mixed in 25 mL CH_2Cl_2 overnight. The mixture was filtered to remove excess NaOH and NaCl. The filtrate was concentrated under reduced pressure and crushed out with

Diethyl ether. The resulting solid was filtered off and air-dried overnight. X-ray quality single crystals (0.21 mmol, 277 mg; yield 65%) were grown by slow diethyl ether vapor diffusion into a CH_2Cl_2 solution of **$(Ph_4P)_2$[1]**.

$[Cu_3(\mu_3\text{-}OH)(\mu\text{-}4\text{-}CH(O)\text{-}pz)_3(\mu\text{-}1,2\text{-}bpe)_2(1,2\text{-}bpe)_2(H_2O)](CF_3SO_3)_2 \cdot 3H_2O$, [2]$(CF_3SO_3)_2$

$Cu(CF_3SO_3)_2$ (0.60 mmol, 225 mg), 4-CH(O)-pzH (0.56 mmol, 53 mg) and NaOH (0.94 mmol, 38 mg) were mixed in 25 mL MeOH. 1,2-bpe (0.96 mmol, 187 mg) was dissolved in 25 mL MeOH and was added dropwise to the Cu salt solution over 2 h. The reaction mixture was stoppered and stirred overnight at room temperature. A small amount of brown precipitate was filtered off and the filtrate was allowed to evaporate slowly to yield blue-green crystals (0.11 mmol, 181 mg; yield 57%) of **[2](CF$_3$SO$_3$)$_2$** over two weeks. Analysis calculated for $C_{62}H_{58}N_{14}Cu_3O_{14}F_6S_2$: C, 46.78; H, 3.67; N, 12.32. Found: C, 46.63; H, 3.66; N, 12.34.

{[Cu$_3$(μ$_3$-OH)(μ-4-CH(O)-pz)$_3$(H$_2$O)$_2$](CF$_3$SO$_3$)$_2$·3.5H$_2$O}$_n$, [3](CF$_3$SO$_3$)$_2$

$Cu(CF_3SO_3)_2$ (1 mmol, 361 mg), 4-CH(O)-pzH (1 mmol, 96 mg) and NaOH (2 mmol, 80 mg) were mixed in 25 mL of pyridine overnight at room temperature. The reaction mixture was filtered and the solvent was removed under reduced pressure. The residue was suspended in 10 mL of THF and filtered (0.08 mmol, 66 mg; yield 24%). X-ray quality dark-blue single crystals of **[3](CF$_3$SO$_3$)$_2$** were obtained after one week

{[Cu$_3$(μ$_3$-OH)(μ-4-CH(O)-pz)$_3$(py)$_3$](CF$_3$SO$_3$)$_2$}$_n$, [4](CF$_3$SO$_3$)$_2$

[4](CF$_3$SO$_3$)$_2$ was an impurity of the synthesis of **[3](CF$_3$SO$_3$)$_2$** and was islated as a few a X-ray quality crystals from the bulk powder of **[3](CF$_3$SO$_3$)$_2$**.

{[Cu$_3$(μ$_3$-OH)(μ-4-CH(O)-pz)$_3$](ClO$_4$)$_2$}$_n$, [5](ClO$_4$)$_2$

[5](ClO$_4$)$_2$ was prepared using the same procedure as **3**, using $Cu(ClO_4)_2·6H_2O$ (1 mmol, 370 mg) instead of $Cu(CF_3SO_3)_2$. X-ray quality crystals were obtained by slow diffusion of diethylether vapor into a THF solution of **[5](ClO$_4$)$_2$** (0.23 mmol, 162 mg; yield 70%).

Crystallography

Crystallographic details on the compounds discussed here are summarized in Table 1. **[2](CF$_3$SO$_3$)$_2$**, **[3]CF$_3$SO$_3$** and **[5](ClO$_4$)$_2$** contained interstitial solvent molecules that were removed using the SQUEEZE protocol available with PLATON.[38] The amount of solvent molecules was determined from a combination TGA and elemental analyses. In **[2](CF$_3$SO$_3$)$_2$**, the (μ$_3$-OH) is located on a C_2-axis and coplanar with the three Cu-atoms. However, its thermal ellipsoid is vertically elongated, indicating that the pyramidal OH-group is disordered among two sites, above and below the Cu_3-plane.

Table 2. Selected interatomic distances (Å) and angles (°)

	[1]$^{2-}$	**[2]$^{2+}$**	**[3]$^{2+}$**	**[4]$^{2+}$**	**[5]$^{2+}$**
Cu-μ$_3$-O(H)	1.887(2)-1.899(2)	1.978(2)-1.986(4)	1.986(3)-2.030(3)	1.981(4)-2.009(4)	2.000(4)
Cu-N	1.948(2)-1.963(2)	1.951(2)-1.984(3)	1.936(4)-1960(4)	1932(5)-2002(4)	1.93(1)
Cu-L	2.283(1)-2.315(1)	2.099(4)	1.982(3), 2.023(3)	2.010(6)-2.017(4)	N/A
Cu-bipy	N/A	2.045(3), 2.493(4)	N/A	N/A	N/A
O-Cu-Bipy	N/A	159.2(1)	N/A	N/A	N/A
O…Cu-plane	N/A	N/A	0.517, 0.534	0.508, 0.567	0.603
Cu-OClO$_3$/trif	N/A	N/A	2.427(5)-2.565(5)	2.19(1)-2.497(7)	2.579(3), 2.726(5)
Cu-O-Cu	118.5(1)-120.7(1)	120.0(1)	110.0(1)-115.5(2)	110.5(2)-118.1(2)	111.1(2)
N-Cu-N	160.3(1)-176.5(1)	169.3(1)-177.3(2)	169.7(2)-179.5(2)	167.8(2)-177.9(2)	175.7(2)
O-Cu-O	N/A	N/A	167.5(1)-175.5(1)	165.5(2)-178.6(2)	171.1(2)
O-Cu-L	158.1(1)-170.3(1)	180.0(1)	174.3(1)-178.6(1)	162.1(2), 178.2(2)	N/A
C=O (Cu-bound)	N/A	N/A	1.239(6), 1.234(6)	1.177(8) – 1.256(8)	1.226(7)
C=O (free)	1.19(2) - 1.204(4)	1.156(6), 1.202(8)	1.183(8), 1.204(7), 1.202(8)	N/A	N/A
(C=O)O-Cu	N/A	N/A	2.020(3)	1.973(4)-2.479(5)	1.982(4)

Results and Discussions

Synthesis

All five compounds form by self-assembly, upon mixing a Cu(II) salt, 4-CH(O)-pzH, NaOH, a counterion and pyridine or 1,2-bpe in an organic solvent. **(Ph$_4$P)$_2$[1]** is the only discrete trinuclear complex with terminal chloride ligands instead of a bridging linker. **[2](CF$_3$SO$_3$)$_2$** was obtained in a soluble form only from a dilute reaction mixture to which the linker was added slowly; Fast addition of the linker forces rapid precipitation of **[2](CF$_3$SO$_3$)$_2$** as an amorphous solid whose composition was determined by elemental analysis. Crystals of **[2](CF$_3$SO$_3$)$_2$** were formed in good yield by slow evaporation of the filtrate. In the structures of **(Ph$_4$P)$_2$[1]** and **[2](CF$_3$SO$_3$)$_2$**, the 4-CH(O) substituents are spectator groups.

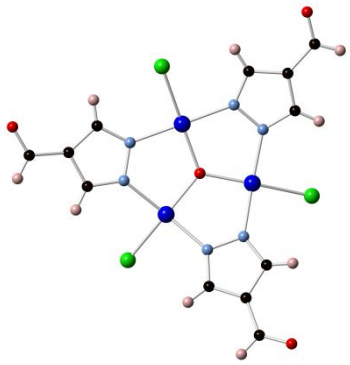

Figure 1. Ball-and-stick diagram of $\mathbf{1}^{2-}$, counter cation omitted for clarity. Color coding: Blue, Cu; red, O; light blue, N; black, C; green, Cl; pink, H.

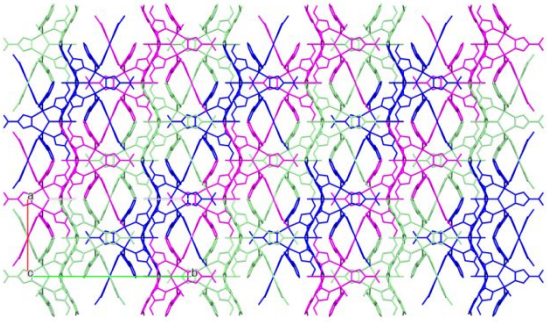

Figure 2. Diagram of three-fold interpenetration of $\mathbf{2}^{2+}$ viewed along the crystallographic *c*-axis. H-atoms and counter anions are not shown for clarity.

In the absence of competing ligands (such as Cl in **$(Ph_4P)_2$[1]** and 1,2-bpe in **[2]$(CF_3SO_3)_2$**), the formyl group participates in completing the coordination sphere of the Cu^{2+}. **[3]$(CF_3SO_3)_2$** is the only 1D-chain in this series of compounds, as two of the three Cu-centers of its trinuclear SBU are terminated by water ligands. In **[4]$(CF_3SO_3)_2$** one of the Cu-centers is terminated by py. Interestingly, **[3]$(CF_3SO_3)_2$** and **[5]$(ClO_4)_2$** formed from reaction mixtures that also contained pyridine, yet no pyridine molecule was coordinated to the Cu centers.

Crystal Structure Descriptions

$(Ph_4P)_2$[1] crystallizes in the triclinic *P-1* space group with the whole trinuclear complex in the asymmetric unit (Fig. 1). Its bond lengths and angles (Table 2) are unexceptional and in agreement with several similar trinuclear Cu(II)-pyrazolates in the literature.[25] The carbonyl C-O bonds are 1.194(1) – 1.204(4) Å long.

[2]$(CF_3SO_3)_2$ crystallizes in the monoclinic *C2/c* space group with one half molecule in the asymmetric unit. A C_2 axis passes through one of the Cu-atoms and the center of a pyrazole ring, bisecting the molecule and imposing a crystallographic disorder on one carbonyl group. The dangling carbonyl groups in this compound are non-coordinating, with typical C-O double bond lengths of 1.156(6) and 1.202(8) Å. The Cu-centers are in 5-coordinate square pyramidal geometry. One of the bidentate bpe ligands links two Cu_3-SBUs and one is terminal (i.e., monodentate, non-catenating). One of the terminal positions is also occupied by a water molecule, which in turn is H-bonded to the non-catenating bpe linker (OH···N distance: 2.802(5) Å). A crystal packing diagram shows parallel

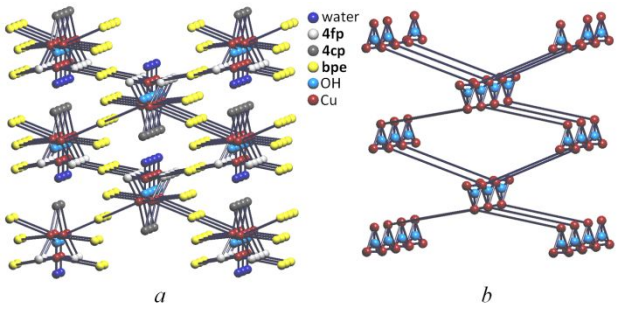

Figure 3. Standard representation of $\mathbf{2}^{2+}$: a) The net obtained after primary simplification; b) The 3,4,5-c underlying net of 3,4,5T174 topological type obtained after secondary simplification procedure.

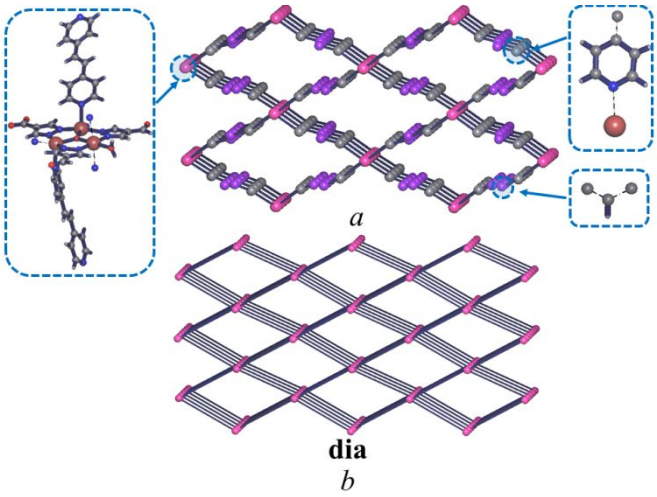

Figure 4. Underlying net of of $\mathbf{2}^{2+}$ obtained by the cluster representation procedure at 6-rings: a) Dissection of the structure by means of the cluster simplification procedure as implemented in ToposPro; b) The 4-c underlying net of **dia** topological type obtained after secondary simplification procedure.

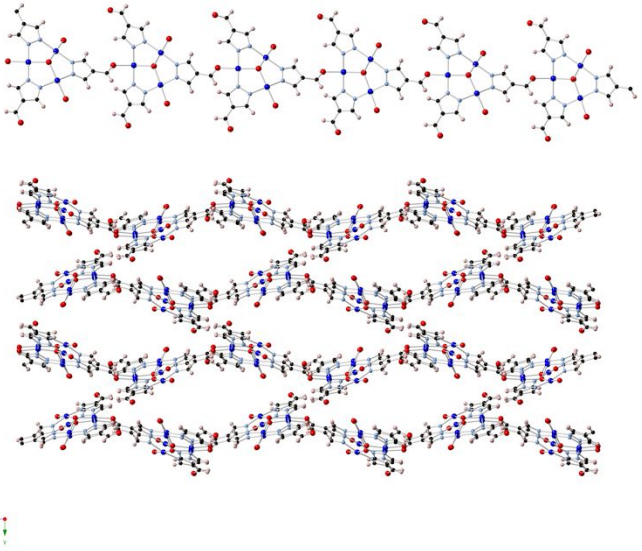

Figure 5. Molecular structures of one of the chains of $\mathbf{3}^{2+}$ (top); Packing diagram showing the wave-like arrangement parallel to the crystallographic *a*-axis (bottom). CF_3SO_3 anions are not shown. Color coding: Blue, Cu; red, O; light blue, N, black, C and pink, H.

pillars along the crystallographic *c*-axis with no π-π interactions between adjacent pyridyl rings of the 1,2-bpe linkers (ring centroid-to-centroid distances: 3.661 and 3.714 Å. In the literature, 1,2-bpe has been reported as a component of pillared structures in some soft-porous materials.[39] In addition to the common 3D network structures in **dia** topology, **[2](CF$_3$SO$_3$)$_2$** is 3-fold interpenetrated (Fig. 2), as is quite common among lattices containing long bis-pyridyl linkers.[40,41] Due to interpenetration, the void volume of this lattice is only 5.8 %. Pairs of adjacent C=C bonds in **[2](CF$_3$SO$_3$)$_2$** are only 3.791(6) Å and 3.603(6) Å apart. Vittal *et al.* have reported SCSC cycloaddition reactions under similar conditions (3.79, 3.77 and 3.99 Å).[42]

Topology of [2](CF$_3$SO$_3$)$_2$

The underlying topology of **[2](CF$_3$SO$_3$)$_2$**, is a 3-nodal 3,4,5-*c* net of 3,4,5T174 topological type (Fig. 3).

The connectivity of the copper clusters in **[2]$^{2+}$** is described by the 4-*c* uninodal net of **dia** topological type (Fig. 4). The MOF structure comprises three interpenetrating networks, which are related by translations along the [100] direction, thus being characterized by interpenetration Class *Ia*.[43]

[3](CF$_3$SO$_3$)$_2$ crystallizes in the monoclinic *P2$_1$/n* space group, with two Cu_3 SBUs in the asymmetric unit, connected via the carbonyl oxygen of the 4-CH(O)-pz ligand forming an 1D chain. two of its three Cu-centers are terminated by water molecules, preventing extension into 2D- or 3D-network (Fig. 5). The overall backbone structure of the Cu_3-units is similar to that found in the literature with other Cu_3N_6 metallacycles and the two μ_3-O(H) are located 0.536(1) and 0.516(1) Å above their respective Cu_3-planes. The Cu-centers are all 5-coordinate in a square pyramidal N_2O_3 environment. Axial coordination is provided by a CF_3SO_3 counter-anion, while pyrazolato-N, μ_3-O and water or the carbonyl-O atoms are in the equatorial plane. As mentioned earlier, carbonyl groups of two (out of six) 4-CH(O)-pz are involved in corrdination, causing elongation of the C-O bond distances of the coordinating carbonyl groups: 1.234(1) Å and 1.239(1) Å, while the C-O bonds of non-coordinating carbonyl groups are shorter than 1.210 Å and close to a typical C-O bond in an aldehyde and also those seen in **1**. While 3D structures are fairly common with Cu_3-pyrazolato subunits, 1D chains and 2D sheets are rather uncommon, with just a few examples in the literature reported by us and others.[40,44–55] The two Cu_3-SBUs differ from each other in that two loosely associated water molecules are coordinated perpendicular to the Cu4-Cu5-Cu6 subunit, whereas the Cu3-Cu4-Cu5 subunit has only one coordinated water molecule.

[4](CF$_3$SO$_3$)$_2$ has a 3D-network structure that crystallizes in the orthorhombic *Pna2$_1$* space group with two Cu_3 SBUs in the asymmetric unit (Fig. 6). The Cu_3N_6 metallacycles have Cu-centers with either a 5-coordinated square pyramidal or a pseudo-octahedral geometry. The axial positions are occupied by triflate ions with bond distances of 2.19(1)-2.497(7) Å. An interesting feature of **[4](CF$_3$SO$_3$)$_2$** is that all carbonyl groups

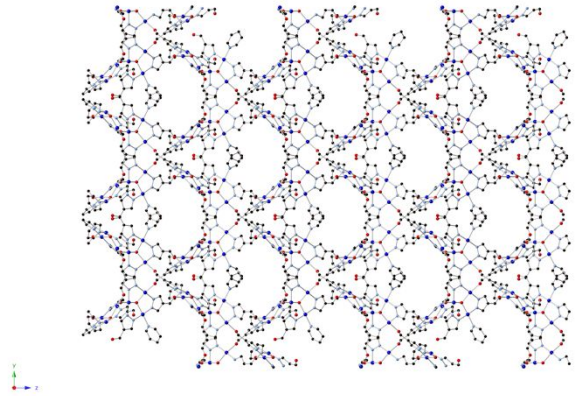

Figure 6. Molecular packing diagram for **4**$^{2+}$ viewed along the crystallographic *a*-axis. Color coding: Blue, Cu; red, O; light blue, N and black, C. H-atoms and counter anions are not shown for clarity.

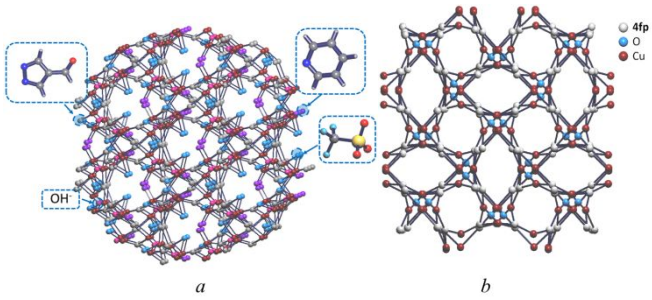

Figure 7. Standard representation of **4**$^{2+}$: a) The 14-nodal $3^8,4^2,5^4$-c net obtained after primary simplification. Red spheres correspond to copper atoms, purple spheres represent hydroxyl anions, grey spheres - 4-CH(O)-pz ligands and violet spheres - pyridine molecule; b) The underlying net of new topological type obtained after secondary simplification procedure.

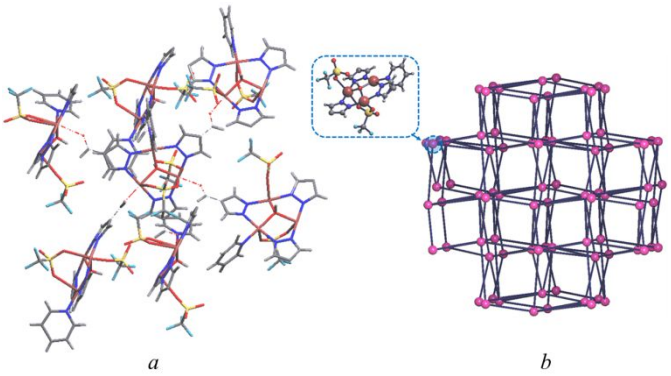

Figure 8. Underlying net of **4**$^{2+}$ obtained by the cluster representation procedure at 6-rings: a) Dissection of the structure to clusters by ToposPro; b) The 6-c underlying net of the **sol** topological type obtained after secondary simplification procedure.

are involved in coordination and all but one C-O distances are over 1.2 Å. The two shorter carbonyl C-O bonds of 1.177(8) Å and 1.179(9) are weakly coordinating at the axial position of Cu atoms at 2.315(5) Å and 2.479(5) Å, respectively. These two bonds are ~0.3-0.4 Å longer than the other CO-Cu bond distances. The shortest CO-Cu bond in **[4](CF$_3$SO$_3$)$_2$** is 1.973(4) Å, far shorter than analogous Cu-OC bonds hitherto reported.[2,20–22] The solvent accessible void volume is 2982.98 Å^3 (29%). The structure differs from that of **[5](ClO$_4$)$_2$** (*vide infra*) in the pyridine coordination. The Cu_3(μ_3-OH)-unit is also

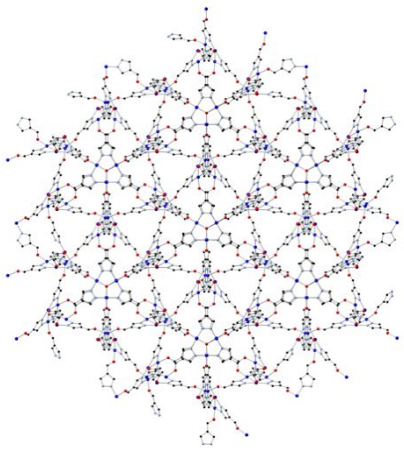

Figure 9. Molecular packing diagram of $\mathbf{5}^{2+}$ viewed along the crystallographic [111] plane. Counter anions and H-atoms are not shown for clarity. Color coding: Blue, Cu; red, O; light blue, N, and black, C.

similar to those found in the literature[28] with the μ_3-O(H)-located 0.560(4) and 0.508(4) Å above the Cu_3-planes.

Topology of $[4](CF_3SO_3)_2$

In the standard simplification procedure,[43] the Cu atoms are shown, while ligands are represented by their centers of mass, keeping the connectivity with their neighbors (Fig. 7a). Upon secondary simplification of the obtained net, by removing of the 0- and 1-coordinated ligands (nodes) and replacing the 2-coordinated ligands (nodes, or bridge structural groups) by net edges. The resulting topology is a 14-nodal $3^8,4^2,5^4$-c net. The point symbol for this net is $\{3.4^2\}_2\{3.8.9\}_2\{3^2.4^2.5.6.8.9.10^2\}_2\{3^2.4^2.5.6.8.9^2.10\}$ $\{3^2.4^2.5.6.8^2.9.10\}\{4.8.10\}\{4.8.9\}\{4.8^2\}_2\{4^2.5.8.10^2\}\{4^2.5.8^2.10\}$, and is not contained in the TOPOS Topological Database. (Fig. 7b).

Using a structure simplification procedure in ToposPro, the $C_{16}H_{12}N_6O_7F_6S_2Cu_3$ were identified as having the connectivity described by the 6-c uninodal net of the **sol** topological type (Fig. 8).[43] There is only one other CP that shows this topology.[56]

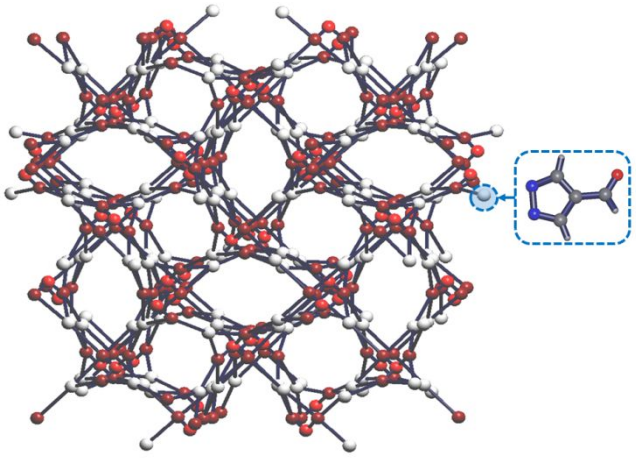

Figure 10. Standard representation of $\mathbf{5}^{2+}$: the 3,3,4-c underlying net of new topological type obtained after secondary simplification procedure.

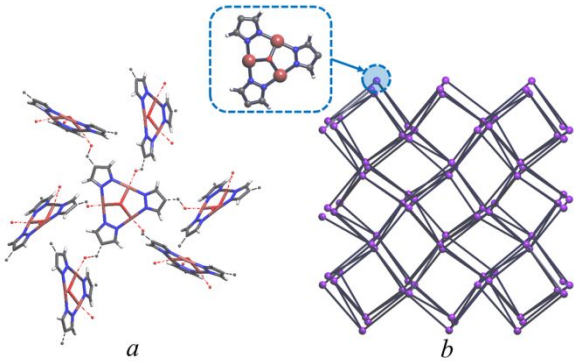

Figure 11. Underlying net of $\mathbf{5}^{2+}$ obtained by the cluster representation procedure at 5-rings: a) Dissection of the structure to clusters by ToposPro; b) The 6-c underlying net of the **bcs** topological type obtained after secondary simplification procedure.

$[5](ClO_4)_2$, another 3D polymer, crystallizes in the highly symmetric cubic space group $I\bar{4}3d$ with the asymmetric unit containing one-third of the Cu_3 SBU, i.e., one Cu^{2+}, one 4-CH(O)-pz$^-$, one-third μ_3-OH^- and two-thirds ClO_4^- counter anion. In the extended structure, all carbonyl groups are involved in Cu-coordination (Fig. 9) with CO-Cu bonds of 1.982(4) Å, the second shortest bond among the structures reported here, and a long C-O bond of 1.226(7) Å. The structure is characterized by six contacts around the Cu_3 SBU, three dative bonds to neighboring SBUs, and three dative bonds from neighboring SBUs. The solvent accessible void volume is 4294.78 Å^3 (31.7%).

Topology of $[5](ClO_4)_2$

After procedure for simplification of the network, described for **$[4](CF_3SO_3)_2$**, a 3-nodal 3,3,4-c net is determined; this connectivity is not encountered in the Topos Topologic Database (Fig. 10). The point symbol for the net is $\{4.8^2\}_3\{4^2.6.8^2.10\}_3\{4^3\}$.

Cluster simplification revealed that the net created by $C_9H_6N_6OCu_3$ clusters is described by the 6-c uninodal net of the **bcs** topological type (Fig. 11).[43] There are two MOFs that display **bcs** topology.[57,58]

Thermogravimetric Analysis

Thermogravimetric analyses of **$[2](CF_3SO_3)_2$**, **$[3](CF_3SO_3)_2$** and **$[5](ClO_4)_2$** indicate that all three release solvent molecules before decomposition. Approximately 5 weight % of **$[2](CF_3SO_3)_2$** is lost at < 95 ºC corresponding to three interstitial water molecules (calc. 3.4%), followed by decomposition at ~230 ºC. Approximately 10 weight % of **$[3](CF_3SO_3)_2$** and **$[5](ClO_4)_2$** is lost at < 95 ºC corresponding to 5.5 H_2O molecules (calc. 11%) and one THF molecule (calc. 9.4%), respectively. Upon further heating, **$[3](CF_3SO_3)_2$** undergoes an additional ~ 10 weight % loss, then decays sharply at 510 °C. **$[5](ClO_4)_2$** behaves similarly to **$[2](CF_3SO_3)_2$** (Fig. S1).

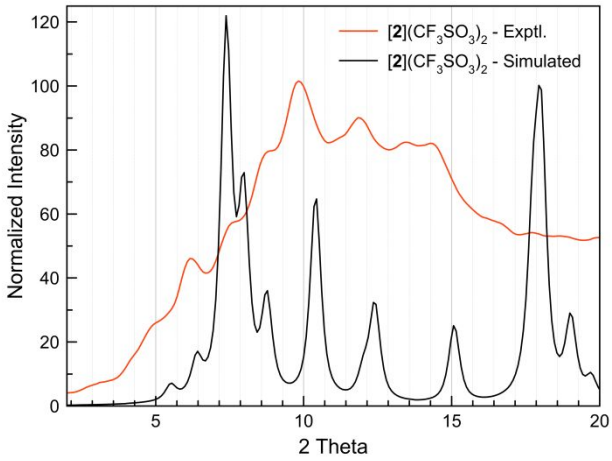

Figure 12. Powder diffraction of **[2](CF$_3$SO$_3$)$_2$**. Red, experimental; black, simulated

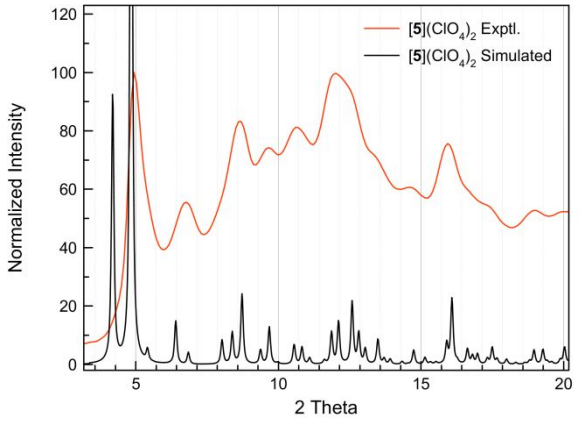

Figure 13. Powder diffraction of **[5](ClO$_4$)$_2$**. Red, experimental; black, simulated

Powder X-ray Diffraction

The powder diffractions of bulk **[2](CF$_3$SO$_3$)$_2$** and **[5](ClO$_4$)$_2$** match well with the simulated patterns (Figs. 12 & S2 and Figs. 13 & S3, respectively).

Single crystals of compounds **[3][CF$_3$SO$_3$]$_2$** (major product) and **[4][CF$_3$SO$_3$]$_2$** (minor product) were isolated from the same reaction mixture. The experimental diffraction pattern of bulk reaction product is a good match to the overlapping simulated patterns of the two components (Fig. S4).

As proof of concept that the synthesis of lattices **3**$^{2+}$ and **5**$^{2+}$ (and presumably also **[4](CF$_3$SO$_3$)$_2$**) can be reversed while maintaining intact the Cu$_3$-SBUs, their dissolution was studied by IR and ^{1}H-NMR spectra were examined. IR data was collected form 4000-500 cm^{-1} using 16 scans. Compound **[3](CF$_3$SO$_3$)$_2$** displays absorptions for both coordinated (1616 cm^{-1}) and uncoordinated (1663 cm^{-1}) carbonyl groups. Upon dissolution in acetonitrile, a slight, but visible, color change occurred and only one carbonyl absorption appeared at 1680 cm^{-1} (Fig S5). **[5](ClO$_4$)$_2$** shows one carbonyl absorption at 1614 cm^{-1}, associated with the coordinated aldehyde. Once **[5](ClO$_4$)$_2$** was dissolved in acetonitrile, this band shifted to

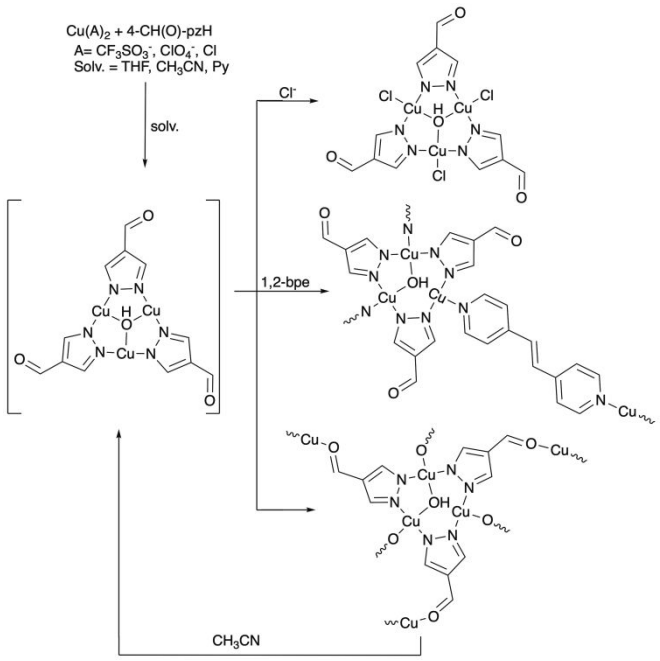

Scheme 1. Reaction pathway determined in the study.

1675 cm^{-1} (Fig. S6), indicating that the aldehyde was no longer coordinated. **[2](CF$_3$SO$_3$)$_2$** is not soluble in MeCN, its IR spectrum showing only the 1668 cm^{-1} absorption corresponding to uncoordinated CH(O) groups (Fig. S7). The NMR spectrum of **[5](ClO$_4$)$_2$** in CD_3CN has two paramagnetically shifted resonances at +37.69 ppm (1H, $w_{1/2}$ = 1033 Hz, C(O)H) and +19.85 ppm (2H, $w_{1/2}$ = 312 Hz, H^{3,5}) corresponding to a Cu$^{II}_3$-pyrazolato complex (Fig S8). The chemical shifts of these resonances are similar to those of analogous Cu_3 compounds we have previously reported,[24] clearly indicating the presence of a trinuclear species in the solution of **[5](ClO$_4$)$_2$**. The paramagnetic shift and broadening are consistent with a strongly antiferromagnetically coupled Cu$^{II}_3$ system, as described in an earlier paper.[25]

Conclusions

The results of this work are summarized in Scheme 1. By reporting the first three CPs based on Cu$_3$-4-formyl pyrazolate metallacycles, we have shown that formyl groups can be exploited as ligands for Cu(II) centers (even in the absence of chelation, such as seen with pyridine-2-carboxaldehyde) and further exploited this property for linking the trinuclear SBUs. The extended network structures exhibit uncommon topologies, such as **sol** and **bcs** (in **4**$^{2+}$ and **5**$^{2+}$, respectively). When competing, stronger-coordinating ligands are present, the aldehyde groups remain free and either linking is accomplished through other bridging ligands (e.g., 1,2-bpe in **2**$^{2+}$), or 0-D Cu$_3$ complexes are formed when terminal ligands (e.g., chlorides in **1**$^{2-}$) are present. Finally, we have shown that the assembly of the Cu$_3$-SBUs into the formyl-linked CPs **3**$^{2+}$ - **5**$^{2+}$ is reversible.

Conflicts of interest

There are no conflicts to declare.

Acknowledgements

Financial support of this work by the National Science Foundation (CHE-1213683) is acknowledged. The authors thank Raquel Cruz for her help with the synthesis of compound **2**. We are grateful to the TOPOSPro team for topology analyses of the 3D structures.

Notes and references

1 B. Müller and H. Vahrenkamp, *Eur. J. Inorg. Chem.*, 1999, **1999**, 137–144.
2 F. Xu, B. Hu, X.-X. Wang, J. Geng and W. Huang, *J. Coord. Chem.*, 2012, **65**, 2201–2210.
3 C. M. Alvarez, R. García-Rodríguez and D. Miguel, *Dalton Trans.*, 2007, 3546.
4 D. Saravanabharathi, M. Nethaji and A. G. Samuelson, *J. Chem. Sci.*, 2002, **114**, 347–356.
5 E. P. Kelson, P. P. Phengsy and A. M. Arif, *Acta Crystallogr. Sect. C*, 2001, **57**, 517–519.
6 T.-Y. Hwang, J.-Y. Cho, M.-K. Jiang and H.-M. Gau, *Inorg. Chim. Acta*, 2000, **303**, 190–198.
7 M. Bochmann, K. J. Webb, M. B. Hursthouse and M. Mazid, *J. Chem. Soc., Chem. Commun.*, 1991, **0**, 1735–1737.
8 H.-M. Gau, C.-S. Lee, C.-C. Lin, M.-K. Jiang, Y.-C. Ho and C.-N. Kuo, *J. Am. Chem. Soc.*, 1996, **118**, 2936–2941.
9 P. G. Cozzi, E. Solari, C. Floriani, A. Chiesi-Villa and C. Rizzoli, *Chem. Ber.*, 1996, **129**, 1361–1368.
10 R. L. Cicero and J. D. Protasiewicz, *Organometallics*, 1995, **14**, 4792–4798.
11 B. Müller, M. Ruf and H. Vahrenkamp, *Angew. Chem. Int. Ed.,* 1994, **33**, 2089–2090.
12 M. P. Byrn, C. J. Curtis, Y. Hsiou, S. I. Khan, P. A. Sawin, S. K. Tendick, A. Terzis and C. E. Strouse, *J. Am. Chem. Soc.*, 1993, **115**, 9480–9497.
13 D. K. Garner, R. A. Allred, K. J. Tubbs, A. M. Arif and L. M. Berreau, *Inorg. Chem.*, 2002, **41**, 3533–3541.
14 Q. Wang, D.-Q. Wang and Y.-Y. Sun, *Acta Crystallogr., Sect. E*, 2007, **63**, m2819–m2819.
15 A. Caneschi, D. Gatteschi and R. Sessoli, *Inorg. Chem.*, 1993, **32**, 4612–4616.
16 B. Müller and H. Vahrenkamp, *Eur. J. Inorg. Chem.*, 1999, **1999**, 117–127.
17 B. Müller and H. Vahrenkamp, *Eur. J. Inorg. Chem.*, 1999, **1999**, 129–135.
18 H. Eklund, B. Nordström, E. Zeppezauer, G. Söderlund, I. Ohlsson, T. Boiwe, B.-O. Söderberg, O. Tapia, C.-I. Brändén and Å. Åkeson, *J. Mol. Biol.,* 1976, **102**, 27–59.
19 G. A. Jeffrey, *An introduction to hydrogen bonding*, Oxford University Press, New York, 1997.
20 J.-L. Zeng, Y.-M. Jiang and K.-B. Yu, *Acta Cryst. Sect. E*, 2003, **59**, m1137–m1139.
21 S. Andersson, M. Håkansson, S. Jagner, M. Nilsson, C. Ullenius, F. Urso, J. Weidlein and R. A. Zingaro, *Acta Chem. Scand. A*, 1986, **40a**, 58–62.
22 D. Xu, J. Geng, Y. Dai, Y.-X. Peng, H.-F. Qian and W. Huang, *Dyes Pigm.*, 2017, **136**, 398–403.
23 C. K. Hartman and G. Mezei, *Inorg. Chem.*, 2017, **56**, 10609–10624.
24 M. Rivera-Carrillo, I. Chakraborty, G. Mezei, R. D. Webster and R. G. Raptis, *Inorg. Chem.*, 2008, **47**, 7644–7650.
25 P. A. Angaridis, P. Baran, R. Boča, F. Cervantes-Lee, W. Haase, G. Mezei, R. G. Raptis and R. Werner, *Inorg. Chem.*, 2002, **41**, 2219–2228.
26 L. Mathivathanan, A. K. Boudalis, P. Turek, M. Pissas, Y. Sanakis and R. G. Raptis, *Phys. Chem. Chem. Phys.*, 2018, **20**, 17234–17244.
27 G. Mezei, J. E. McGrady and R. G. Raptis, *Inorg. Chem.*, 2005, **44**, 7271–7273.
28 C. Pettinari, N. Masciocchi, L. Pandolfo and D. Pucci, *Chem. -Eur. J.*, 2010, **16**, 1106–1123.
29 K. Shi, L. Mathivathanan, V. A. Drozd and R. G. Raptis, *Cryst. Growth Des.*, 2019, **19**, 381–390.
30 G. M. Sheldrick, *Acta Crystallogr. Sect. A*, 2015, **71**, 3–8.
31 G. M. Sheldrick, *Acta Cryst. Sect. C*, 2015, **71**, 3–8.
32 O. V. Dolomanov, L. J. Bourhis, R. J. Gildea, J. a. K. Howard and H. Puschmann, *J. Appl. Cryst.*, 2009, **42**, 339–341.
33 A. P. Hammersley, S. O. Svensson and A. Thompson, *Nuclear Instruments and Methods in Physics Research Section A: Accelerators, Spectrometers, Detectors and Associated Equipment*, 1994, **346**, 312–321.
34 A. P. Hammersley, S. O. Svensson, M. Hanfland, A. N. Fitch and D. Hausermann, *High Press. Res.*, 1996, **14**, 235–248.
35 V. A. Blatov, A. P. Shevchenko and D. M. Proserpio, *Cryst. Growth Des.,* 2014, **14**, 3576-3586.
36 C. F. Macrae, I. J. Bruno, J. A. Chisholm, P. R. Edgington, P. McCabe, E. Pidcock, L. Rodriguez-Monge, R. Taylor, J. van de Streek and P. A. Wood, *J. Appl. Cryst.*, 2008, **41**, 466–470.
37 F. Menges, *Spectragryph*, .
38 A. L. Spek, *Acta Crystallogr. Sect. D*, 2009, **65**, 148–155.
39 S. Kitagawa, R. Kitaura and S. Noro, *Angew. Chem. Int. Ed.*, 2004, **43**, 2334–2375.
40 L. Mathivathanan, J. Torres-King, J. N. Primera-Pedrozo, O. J. García-Ricard, A. J. Hernández-Maldonado, J. A. Santana and R. G. Raptis, *Cryst. Growth Des.*, 2013, **13**, 2628–2635.
41 C. Di Nicola, F. Garau, M. Gazzano, M. F. C. Guedes da Silva, A. Lanza, M. Monari, F. Nestola, L. Pandolfo, C. Pettinari and A. J. L. Pombeiro, *Cryst. Growth Des.*, 2012, **12**, 2890–2901.
42 M. H. Mir, L. L. Koh, G. K. Tan and J. J. Vittal, *Angew. Chem. Int. Ed. Engl.*, 2010, **49**, 390–393.
43 E. V. Alexandrov, V. A. Blatov, A. V. Kochetkov and D. M. Proserpio, *CrystEngComm*, 2011, **13**, 3947.
44 S.-Z. Zhan, M. Li, S. W. Ng and D. Li, *Chem. -Eur. J.*, 2013, **19**, 10217–10225.
45 L. Hou, W.-J. Shi, Y.-Y. Wang, H.-H. Wang, L. Cui, P.-X. Chen and Q.-Z. Shi, *Inorg. Chem.*, 2011, **50**, 261–270.
46 M. Casarin, C. Corvaja, C. Di Nicola, D. Falcomer, L. Franco, M. Monari, L. Pandolfo, C. Pettinari and F. Piccinelli, *Inorg. Chem.*, 2005, **44**, 6265–6276.
47 C. Di Nicola, E. Forlin, F. Garau, M. Gazzano, A. Lanza, M. Monari, F. Nestola, L. Pandolfo, C. Pettinari, A. Zorzi and F. Zorzi, *Cryst. Growth Des.*, 2013, **13**, 126–135.
48 C. Di Nicola, F. Garau, M. Gazzano, A. Lanza, M. Monari, F. Nestola, L. Pandolfo and C. Pettinari, *Cryst. Growth Des.*, 2015, **15**, 1259–1272.
49 M. Rivera-Carrillo, I. Chakraborty and R. G. Raptis, *Cryst. Growth Des.*, 2010, **10**, 2606–2612.

50 M. Grzywa, D. Denysenko, A. Schaller, A. Kalytta-Mewes and D. Volkmer, *CrystEngComm*, 2016, **18**, 7883–7893.
51 S. Contaldi, C. Di Nicola, F. Garau, Y. Y. Karabach, L. M. D. R. S. Martins, M. Monari, L. Pandolfo, C. Pettinari and A. J. L. Pombeiro, *Dalton Trans.*, 2009, 4928.
52 R. M. Almotawa, G. Aljomaih, D. V. Trujillo, V. N. Nesterov and M. A. Rawashdeh-Omary, *Inorg. Chem.*, 2018, **57**, 9962–9976.
53 F. Condello, F. Garau, A. Lanza, M. Monari, F. Nestola, L. Pandolfo and C. Pettinari, *Cryst. Growth Des.*, 2015, **15**, 4854–4862.
54 S. Massignani, R. Scatena, A. Lanza, M. Monari, F. Condello, F. Nestola, C. Pettinari, F. Zorzi and L. Pandolfo, *Inorg. Chim. Acta*, 2017, **455**, 618–626.
55 C. Di Nicola, E. Forlin, F. Garau, A. Lanza, M. M. Natile, F. Nestola, L. Pandolfo and C. Pettinari, *J. Organomet. Chem.,* 2012, **714**, 74–80.
56 K. S. Asha, R. Bhattacharjee and S. Mandal, *Angew. Chem. Int. Ed. Engl.*, 2016, **55**, 11528–11532.
57 J. Lefebvre, D. Chartrand and D. B. Leznoff, *Polyhedron*, 2007, **26**, 2189–2199.
58 H. Feuchter, G. Ortiz, Y. Rousselin, A. Bessmertnykh-Lemeune and S. Brandès, *Cryst. Growth Des.*, 2017, **17**, 3665–3676.

Two novel topologies were obtained by self-assembly of 4-formylpyrazolate-Cu_3 SBUs in the absence of competing terminal ligands.